Journal of Robotics and Control (JRC)
Volume 5, Issue 6, 2024
ISSN: 2715-5072, DOI: 10.18196/jrc.v5i6.24073

Optimal Backstepping and Feedback Linearization Controllers Design for Tracking Control of Magnetic Levitation System: A Comparative Study

Fatin R. Al-Ani [1*], Omar F. Lutfy [2], Huthaifa Al-Khazraji [3]
[1, 2, 3] Control and Systems Engineering Department, University of Technology- Iraq, Baghdad 10066, Iraq
Email: [1] cse.22.15@grad.uotechnology.edu.iq, [2] omar.f.lutfy@uotechnology.edu.iq, [3] 60141@uotechnology.edu.iq
*Corresponding Author

***Abstract*—In this paper, the stabilization and trajectory tracking of the magnetic levitation (Maglev) system using optimal nonlinear controllers are considered. Firstly, the overall structure and physical principle represented by the nonlinear differential equations of the Maglev system are established. Then, two nonlinear controllers, including backstepping control (BSC) and feedback linearization (FL), are proposed to force the position of the ball in the Maglev system to track a desired trajectory. In terms of designing the control law of the BSC, the Lyapunov function is utilized to guarantee an exponential convergence of the tracking error to zero. For developing the control law of the FL, an equivalent transformation to convert the nonlinear system into a linear form is used, and then, the state feedback controller (SFC) method is utilized to track the ball to the desired position. In order to obtain a higher accuracy in motion control of the ball, the gains' selection for the controllers to reach the desired response is achieved using the swarm bipolar algorithm (SBA) based on the integral time absolute error (ITAE) cost function. Computer simulations are conducted to evaluate the performance of the proposed methodology, and the results prove that the proposed control strategy is effective not only in stabilizing the ball but also in rejecting the disturbance present in the system. However, the BSC exhibits better performance than that of the FL-SFC in terms of reducing the ITAE index and improving the transit response even when the external disturbance is applied. The numerical results show that the settling time reduced to 0.2 seconds compared to 1.2 seconds for FL-SFC. Moreover, the ITAE index is reduced to 0.0164 compared to 0.2827 seconds for FL-SFC. In the context of external disturbance, the findings demonstrate that BSC reduced the recovery time to 0.05 seconds compared to 0.65 seconds for FL-SFC.**

Keywords—Magnetic Levitation System; Backstepping Control; Feedback Linearization; State Feedback Controller; Swarm Bipolar Algorithm.

I. INTRODUCTION

Magnetic levitation (Maglev) systems have numerous industrial applications because of their contactless and frictionless properties that increase efficiency and reduce mechanical wear out and maintenance costs [1]-[6]. The system consists of a ferromagnetic ball with a specific amount of mass. The object is suspended in the air gap using the force exerted by the magnetic field whose strength can be controlled through the applied voltage [7]-[10]. Due to its inherent nonlinearities and highly unstable nature, designing a control algorithm that can maintain stable control of the Maglev system is challenging. In this context, many linear and nonlinear controllers have been proposed to stabilize the system.

For instance, Ahmad et al. [11] designed a Proportional-Integral-Derivative (PID) controller for Maglev system. In order to achieve the optimal performance indices, the tuning parameters of the PID controller were tuned using the Genetic Algorithm (GA). Compared to the conventional Ziegler-Nichols (ZN) tuning method, the simulation results revealed that the performance of the PID controller was better than that tuned by the conventional ZN method. Moreover, A. M. Benomair. [12] suggests an optimal linear quadratic regulator by utilizing an enhanced spiral dynamic algorithm for the active control of a magnetic levitation system with full-state feedback linearization. Simulations conducted using the nonlinear mathematical model of the Maglev system demonstrates that the proposed linearization and control approach yield effective results. In the same manner, Roy et al. [13] presented a comparative study between the FOPID controller and the classical PID controller to control the position of the ball in the Maglev system. Three swarm optimizing algorithms were employed, namely, the Gravitational Search Algorithm (GSA), the Particle Swarm Optimization (PSO), and a hybrid algorithm combining both of them, called (PSOGSA), to tune the parameters of the controllers. The outcomes obtained using a wide variety of test signals proved that the PSOGSA hybrid algorithm achieved better results than those of the standalone algorithms. Besides, the performance of the FOPID controller was superior to that of the PID controller. Furthermore, Ataşlar-Ayyildiz and Karahan [14] introduced a PID-like robust fuzzy logic controller (Fuzzy-PID) to improve the system dynamics and stability of the Maglev system. The Cuckoo Search (CS) algorithm was proposed to optimize the controller's parameters using time domain response characteristics as an objective function. Simulation experiments were conducted to evaluate the controller's performance under various conditions, including load disturbances and reference changes. The results indicated that the CS-based Fuzzy-PID controller outperforms the traditional FOPID and the PID controllers in terms of steady-state error, settling time, and overshoot, while also requiring less control effort. In another work, Ekinci et al. [15] proposed a PID plus second-order derivative (PIDD2) controller for the Maglev system. A novel metaheuristic

algorithm named the Manta ray foraging optimization (MRFO) algorithm, together with the generalized opposition-based learning (GOBL) technique and Nelder–Mead (NM) simplex search method, was exploited to attain the optimum values of the design variables for the proposed controller. In addition, Chiem and Thang [16] presented a linear feedforward control method combined with a fuzzy logic controller (FLC) for the Maglev system. The proposed controller ensured the stability of the ball and increased the system's fast-response when the ball deviates from equilibrium. The performance of the proposed control algorithm was compared with that of the conventional PID controller and the standalone FLC. The results showed a fast and stable response even in the presence of noise. However, the limitation of the aforementioned studies is that they considered the linear model of the Maglev system.

In terms of designing a controller for the nonlinear model of the Maglev system, Al-Muthairi and Zribi [17] proposed a sliding mode control (SMC) method to guarantee the asymptotic regulation of the states of the Maglev system to their desired values. To minimize the chattering problem, two modifications of the SMC were made. The robustness of the developed control schemes to variations in the parameters of the system was investigated, and it was found that the control schemes are robust to parameter variations. Another application of the SMC to the Maglev system was achieved by Ma'arif et al. [18]. The system controlled by SMC has a fast output response with no steady-state error. However, the authors did not provide a solution to the chattering problem in the study. In another work, Uswarman et al. [19] presented a comparative study between the conventional SMC (CSMC) and the SMC with gain-scheduling. The simulation results showed that the SMC with gain-scheduling performed better than the CSMC against external disturbances. However, the chattering problem in both controllers still exists. In light of reviewing the existing literature on the Maglev nonlinear model, it can be observed that the authors employed the SMC in designing the controller. On the other hand, the contributions of the current study can be listed as follows:

- Two nonlinear controllers, including backstepping control (BSC) and feedback linearization-based state feedback controller (FL-SFC) are proposed for the stabilization and trajectory tracking of the Maglev system utilizing the nonlinear model of the system under numerous operations.
- The Lyapunov theory is used for the stability analysis of the proposed controllers.
- The swarm bipolar algorithm is proposed to optimally tune the design parameters of the proposed controllers to improve the dynamic performance of the system.

II. MATHEMATICAL MODEL

The magnetic levitation (Maglev) system consists of a ferromagnetic ball suspended in a voltage-controlled magnetic field [20]. The objective of the Maglev control system is to achieve high accuracy in positioning the small steel ball in a steady position at a stable levitation [21]. The schematic of the maglev system is illustrated in Fig. 1 [18]. Specifically, the parameters of the system with their symbols are the electromagnetic force (fe), the gravitational force (fg), the inductance (L), the resistance (R), the object position (x), the source voltage (V), the object mass (m), and the current (i).

The dynamics of the Maglev mechanical parts can be expressed based on the second Newton law of motion as follows [10]:

$$m\frac{d^2x}{dt^2} = fg - fe \tag{1}$$

where the electromagnetic force and the gravitational force are expressed as:

$$fg = mg \tag{2}$$

$$fe = \frac{1}{2}i^2\frac{d}{dx}\big(L(x)\big) \tag{3}$$

The function L(x) is a nonlinear function that can be represented as:

$$L(x) = L + L_0x_0 \tag{4}$$

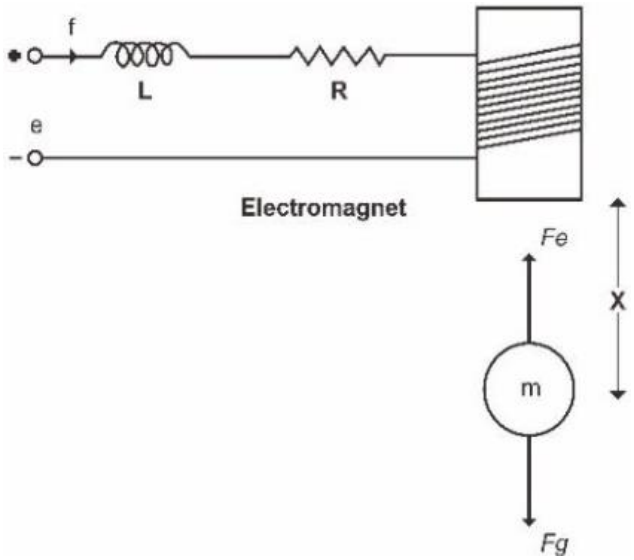

Fig. 1. The maglev system

Equation (4) can be approximated as [17]:

$$L(x) = \frac{2k}{x^2} \tag{5}$$

where k is the force constant. Substituting Eq. (5) in Eq. (3) gives:

$$fe = k\left(\frac{i}{x}\right)^2 \tag{6}$$

Substituting Eq. (2) and (6) in Eq. (1) gives:

$$m\frac{d^2x}{dt^2} = mg - k\left(\frac{i}{x}\right)^2 \tag{7}$$

By rearranging Eq. (7), we get:

$$\frac{d^2x}{dt^2} = g - \frac{k}{m}\left(\frac{i}{x}\right)^2 \tag{8}$$

Besides the mechanical analysis, the Kirchhoff law of voltage in the electrical system can be used to generate Eq. (9).

$$e = iR + \frac{d}{dt}\,L(x)i \tag{9}$$

Using simple mathematical operations, the equation can be rewritten as:

$$\frac{di}{dt} = -\frac{R}{Li} - \frac{2k}{L}\frac{i}{x^2}\frac{dx}{dt} + \frac{1}{L}e \tag{10}$$

By assuming that the states of the system are $x_1 = x, x_2 = \frac{dx}{dt}, x_3 = i$, and the control input to the system is $u = e$, the nonlinear differential equations that capture the dynamics of the Maglev system can be represented as shown below:

$$\frac{dx_1}{dt} = x_2 \tag{11}$$

$$\frac{dx_2}{dt} = g - \frac{kx_3^2}{mx_1^2} \tag{12}$$

$$\frac{dx_3}{dt} = -\frac{Rx_3}{L} + \frac{2kx_2x_3}{Lx_1^2} + \frac{u}{L} \tag{13}$$

where $x_1 > 0$ and $x_3 > 0$. The system's output can be described as:

$$y = x_1 \tag{14}$$

In particular, the nonlinearity features are visible in Eq. (12) and Eq. (13), as can be noticed in the dynamics of the Maglev system. To design the controller, the model of the Maglev is transformed into an equivalent canonical form, which is a more straightforward model that exhibits the nonlinearity using only one dynamic equation. The definition of the nonlinear transformation in coordinates is as follows:

$$z_1 = x_1 \tag{15}$$

$$z_2 = x_2 \tag{16}$$

$$z_3 = g - \frac{kx_3^2}{mx_1^2} \tag{17}$$

Thus, the equivalent model in the new coordinates can be expressed as:

$$\dot{z}_1 = z_2 \tag{18}$$

$$\dot{z}_2 = z_3 \tag{19}$$

$$\dot{z}_3 = f(z) + g(z)\,u \tag{20}$$

where

$$f(z) = \frac{2kR\,x_3^2}{mx_1^2L} - \frac{4k^2\,x_3^2x_2}{mx_1^4L} + \frac{2kx_2x_3^2}{mx_1^3} \tag{21}$$

$$g(z) = -\frac{2kx_3}{mx_1^2L} \tag{22}$$

III. CONTROLLER DESIGN

The utilization of feedback controllers is constantly expanding to control a wide range of systems [22]-[28]. Particularly, controlling the Maglev system involves addressing a range of issues, such as tracking control and handling external disturbances. In this regard, this section explores two nonlinear control strategies to generate the control law for the Maglev system, including the backstepping control (BSC) and the feedback linearization-based state feedback controller (FL-SFC).

A. Backstepping Control

BSC is a control technique that can be applied to various dynamical systems, especially for nonlinear dynamical systems, to obtain a stable control model. In brief, the BSC is a recursive and systematic control process that employs the Lyapunov function to design the control law [29]-[31]. More precisely, to design the BSC, we define e_1 as the error between the actual and the desired outputs:

$$e_1 = z_r - z_1 \tag{23}$$

Taking the derivative of the error gives:

$$\dot{e}_1 = \dot{z}_r - z_2 \tag{24}$$

Moreover, z_2 is selected as the virtual control v_1, which is substituted in Eq. (24) to attain:

$$\dot{e}_1 = \dot{z}_r - v_1 \tag{25}$$

The first Lyapunov function is selected as:

$$V_1 = \frac{1}{2}{e_1}^2 \tag{26}$$

By taking the derivative of V_1, we get:

$$\dot{V}_1 = e_1\dot{e}_1 = e_1(\dot{z}_r - v_1) \tag{27}$$

The virtual control v is selected as:

$$v_1 = \dot{z}_r + \lambda_1 e_1 \tag{28}$$

where $\lambda_1 > 0$,

Substituting v_1 in Eq. (24) gives:

$$\dot{V}_1 = -\lambda_1 {e_1}^2 \tag{29}$$

We define e_2 as the error between the virtual control v_1 and z_2

$$e_2 = z_2 - v_1 \tag{30}$$

Substituting v_1 in Eq. (30) and z_2 in Eq. (24) gives:

$$e_2 = z_2 - \dot{z}_r - \lambda_1 e_1 \tag{31}$$

Substituting z_2 in Eq. (24) gives:

$$\dot{e}_1 = -e_2 - \lambda_1 e_1 \tag{32}$$

By taking the derivative of e_2, we get:

$$\dot{e}_2 = z_3 - \ddot{z}_r - \lambda_1\dot{e}_1 \tag{33}$$

z_3 is selected as the virtual control v_2.

Substituting v_2 in Eq. (33) gives:

$$\dot{e}_2 = v_2 - \ddot{z}_r - \lambda_1\dot{e}_1 \tag{34}$$

The second Lyapunov function is selected as:

$$V_2 = \frac{1}{2}{e_1}^2 + \frac{1}{2}{e_2}^2 \quad (35)$$

By taking the derivative of V_2, we attain:

$$\dot{V}_2 = e_1\dot{e}_1 + e_2\dot{e}_2 \quad (36)$$

Substituting Eq. (33) and Eq. (32) in Eq. (36) gives:

$$\dot{V}_2 = e_1(-e_2 - \lambda_1 e_1) + e_2(v_2 - \ddot{z}_r - \lambda_1\dot{e}_1) \quad (37)$$

Rearranging Eq. (37) gives:

$$\dot{V}_2 = -\lambda_1{e_1}^2 + e_2(-e_1 + v_2 - \ddot{z}_r - \lambda_1\dot{e}_1) \quad (38)$$

The virtual control v_2 is selected as:

$$v_2 = -\lambda_2 e_2 + \lambda_1\dot{e}_1 + e_1 + \ddot{z}_r \quad (39)$$

where $\lambda_2 > 0$

Substituting v_2 in Eq. (38) gives:

$$\dot{V}_2 = -\lambda_1{e_1}^2 - \lambda_2{e_2}^2 \quad (40)$$

Define e_3 as the error between the virtual control v_2 and z_3:

$$e_3 = z_3 - v_2 \quad (41)$$

Substituting v_2 in Eq. (41) gives:

$$e_3 = z_3 + \lambda_2 e_2 - \lambda_1\dot{e}_1 - e_1 - \ddot{z}_r \quad (42)$$

Substituting z_3 in Eq. (33) gives:

$$\dot{e}_2 = -\lambda_2 e_2 + e_3 + e_1 \quad (43)$$

By taking the derivative of e_3, we obtain:

$$\dot{e}_3 = f(z) + g(z)u + \lambda_2\dot{e}_2 + \lambda_1\dot{e}_2 + \lambda_1^2\dot{e}_1 - \dot{e}_1 - \dddot{z}_r \quad (44)$$

Choosing the first Lyapunov function and taking the derivative give:

$$V_3 = \frac{1}{2}{e_1}^2 + \frac{1}{2}{e_2}^2 + \frac{1}{2}{e_3}^2 \quad (45)$$

$$\dot{V}_3 = e_1\dot{e}_1 + e_2\dot{e}_2 + e_3\dot{e}_3 \quad (46)$$

Substituting $\dot{e}_1$, $\dot{e}_2$ and $\dot{e}_3$ gives:

$$\begin{aligned}\dot{V}_3 = {} & e_1(-e_2 - \lambda_1 e_1) + e_2(-\lambda_2 e_2 + e_3 + e_1) \\ & + e_3(f(x) + g(x)u + \lambda_2\dot{e}_2 \\ & + \lambda_1\dot{e}_2 + \lambda_1^2\dot{e}_1 - \dot{e}_1 - \dddot{z}_r)\end{aligned} \quad (47)$$

Rearranging Eq. (47) gives:

$$\begin{aligned}\dot{V}_3 = {} & -\lambda_1{e_1}^2 - \lambda_2{e_2}^2 \\ & + e_3(f(x) + g(x)u + \lambda_2\dot{e}_2 \\ & + \lambda_1\dot{e}_2 + \lambda_1^2\dot{e}_1 - \dot{e}_1 - \dddot{z}_r)\end{aligned} \quad (48)$$

Then, u is selected as follows:

$$\begin{aligned}u_{bsc} = \frac{1}{g(x)}(& -f(x) - \lambda_2\dot{e}_2 - \lambda_1\dot{e}_2 - \lambda_1^2\dot{e}_1 - e_2 \\ & + \dot{e}_1 - \dddot{z}_r - \lambda_3 e_3)\end{aligned} \quad (49)$$

where $\lambda_3 > 0$

Substituting u in Eq. (47) gives;

$$\dot{V}_3 = -\lambda_1{e_1}^2 - \lambda_2{e_2}^2 - \lambda_3{e_3}^2 \quad (50)$$

B. Feedback Linearization-Based State Feedback Controller

One of the well-researched strategies for designing trajectory tracking controllers for nonlinear systems is the feedback linearization (FL) approach [32]-[35]. The control law in FL is designed such that the nonlinear system is transformed into an equivalent linear form as follows:

$$u_{fl} = \frac{1}{g(x)}(-f_X + u_l) \quad (51)$$

where u_l can be any linear controller. In this paper, a state feedback controller (SFC) is selected as follows:

$$u_l = k_1(z_r - z_1) - k_2 z_2 - k_3 z_3 \quad (52)$$

where k_1, k_2 and k_3 are the SFC gains that are designed such that the desired tracking performance is achieved.

C. Swarm Optimization

Swarm optimization algorithms are essential techniques for solving numerous complex problems [36]-[45]. Unlike the trial-and-error method, most of the recent studies formulated the tuning process of the controllers' design variables as an optimization problem. Then, an optimization technique is proposed to solve it [46-49]. In this direction, the problem of tuning the design variables of the BSC and the FL is solved by the swarm bipolar algorithm (SBA), which is a recent swarm optimization technique introduced in [50].

In particular, the SBA is a unique method that splits a swarm into two equal sub-swarms (i.e., one-half of the population is allocated to one sub-swarm, while the other half is assigned to the second sub-swarm). During the initialization phase, all swarm members are distributed throughout the search space. Then, the population is divided into two equal sub-groups. This division is random and not based on the positions of the swarm members in the search space, allowing for a mix of individuals from both sub-swarms. Moreover, SBA makes use of four key references: the best swarm member, the best sub-swarm member, the midpoint between the two best sub-swarm members, and a randomly chosen member from the opposite sub-swarm. These references guide the directed search operations carried out by each swarm member in the iteration process [50]. As the swarm progresses towards the best swarm member, the paths are adjusted to converge towards a specific region. With time, the swarm distribution polarizes into two distinct clusters, moving towards the midpoint between the two best sub-swarm members.

The illustration of these four search operations is presented in Fig. 2. Algorithm 1 presents the pseudo code that formalizes SBA. The procedure of the SBA is mathematically formulated using Eq. (53) to Eq. (62). Specifically, Eq. (53) to Eq. (56) are applied at the startup stage. The uniform distribution is utilized to generate the initial solution of the swarm members, as given in Eq. (53). The rigorous acceptance role used to update the best swarm member is represented by Eq. (54). The first-best sub-swarm member is updated using Eq. (55), while the second-best sub-swarm member is updated using Eq. (56) [50].

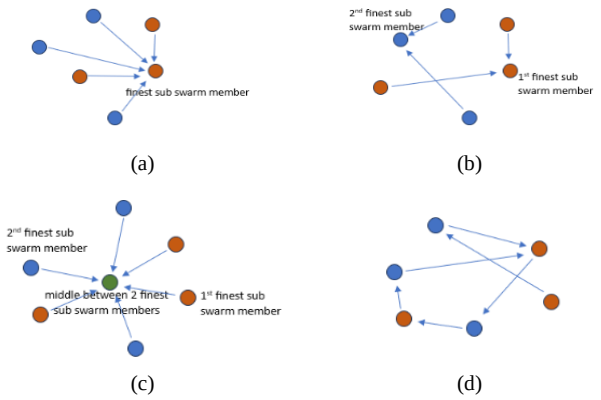

Fig. 2. Illustration of four search operations: (a) first search, (b) second search, (c) third search, and (d) fourth search

Algorithm 1. Pseudo code of SBA

1. **Begin**
2. **For each s ∈ S do**
3. **Generate** the initial solution using Eq. (53)
4. **Update** $s_b$and s_{sb} using Eq. (54) to Eq. (56)
5. **End For**
6. **For** $t = 1$ to t_m do
7. **For each s ∈ S do**
8. **First** search using Eq. (57) and Eq. (58)
9. **Update** $s_b$and s_{sb} using Eq. (54) to Eq. (56)
10. **Second** search using Eq. (59) and Eq. (58)
11. **Update** $s_b$and s_{sb} using Eq. (54) to Eq. (56)
12. **Third** search using Eq. (60) and Eq. (58)
13. **Update** $s_b$and s_{sb} using Eq. (54) to Eq. (56)
14. **Fourth** search using Eq. (61), Eq. (62), Eq. (58)
15. **Update** $s_b$and s_{sb} using Eq. (54) to Eq. (56)
16. **End For**
17. **End For**
18. **Return** s_b
19. **End**

The notations of the SBA are listed below:

d	Dimension
F	objective function
I	index for swarm member
J	index for dimension
S	swarm member
S	swarm/population
s_l	lower boundary
s_u	upper boundary
s_b	the best swarm member
s_{sb}	the best sub swarm member
s_t	randomly picked swarm member
r_1	floating point uniform random [0, 1]
r_2	integer uniform random [1, 2]
T	Iteration
t_m	maximum iteration
U	uniform random

$$s_{i,j} = s_{l,j} + r_1\left(s_{u,j} - s_{l,j}\right) \quad (53)$$

$$s_b = \begin{Bmatrix} s_i, f(s_i) < f(s_b) \\ s_b, else \end{Bmatrix} \quad (54)$$

$$s_{sb1} = \begin{Bmatrix} s_i, f(s_i) < f(s_{sb1}) \ \wedge 1 \le i \le \dfrac{n(s)}{2} \\ s_{sb1}, else \end{Bmatrix} \quad (55)$$

$$s_{sb2} = \begin{Bmatrix} s_i, f(s_i) < f(s_{sb2}) \ \wedge \dfrac{n(s)}{2} < i < n(s) \\ s_{sb2}, else \end{Bmatrix} \quad (56)$$

Equation (57) to Eq. (62) present the mathematical equations during the improvement process. The initial search involves finding the best swarm member according to Eq. (57). The rigorous acceptance role in accepting the candidate solution to replace the swarm member's existing value is represented by Eq. (58). The second search's candidate solution is produced by Eq. (59), in which each sub-swarm member travels in the direction of its own best sub-swarm member. In the third search, all swarm members migrate toward the midpoint between the two best sub-swarm members using Eq. (60). Next, the randomly selected swarm member from the opposing sub-swarm is defined by Eq. (61). Subsequently, the fourth search's movement is represented by Eq. (62), which is dependent on the swarm member's quality comparison and its reference [50].

$$c_{i,j} = s_{b,j} + r_1\left(s_{b,j} - r_2 s_{i,j}\right) \quad (57)$$

$$s_i' = \begin{Bmatrix} c_i, f(c_i) < f(s_i) \\ s_i, else \end{Bmatrix} \quad (58)$$

$$c_{i,j} = \begin{Bmatrix} s_{i,j} + r_1\left(s_{sb1,j} - r_2 s_{i,j}\right), \wedge 1 \le i \le \dfrac{n(s)}{2} \\ s_{i,j} + r_1\left(s_{sb2,j} - r_2 s_{i,j}\right), \wedge \dfrac{n(s)}{2} < i < n(S) \end{Bmatrix} \quad (59)$$

$$c_{i,j} = s_{b,j} + r_1\left(\frac{s_{sb1,j} + s_{sb2,j}}{2} - r_2 s_{i,j}\right) \quad (60)$$

$$s_t = \begin{Bmatrix} U\left(s_1, \dfrac{s_{n(s)}}{2}\right), \dfrac{n(s)}{2} < i < n(S) \\ U\left(s_1, \dfrac{s_{n(s)}}{2}\right), 1 \le i \le \dfrac{n(s)}{2} \end{Bmatrix} \quad (61)$$

$$c_{i,j} = \begin{Bmatrix} s_{i,j} + r_1\left(s_{t,j} - r_2 s_{i,j}\right), f(s_t) < f(s_i) \\ s_{i,j} + r_1\left(s_{i,j} - r_2 s_{t,j}\right), else \end{Bmatrix} \quad (62)$$

IV. Simulation Resuts

In this section, computer simulations are carried out to evaluate the effectiveness of the proposed control strategy. The results are further analyzed to assess their comparative performance. The simulation process of the Maglev system with BSC and FL_FLC was conducted using the Matlab software. The parameters of the Maglev system are listed in Table I [12]. In addition, the initial position of the ball was set to 1 mm, and the desired position was 5 cm.

TABLE I. Parameters of the Maglev System

Parameters	Values
Mass (m)	0.0221 Kg
Inductance (L)	0.02 H
Resistance (R)	4.2 Ω
Force constant (k)	8.25×10-5 Nm2/A2
Gravity acceleration (g)	9.81 m/s2

To ensure the best performance of each controller, the SBA is employed to tune the design parameters of each controller. The performances of the BSC and the FL-SFC are optimized by tuning the adjustable parameters $(\lambda_1, \lambda_2, and\ \lambda_3)$ and $(k_1, k_2, and\ k_3)$ of the control laws given in Eq. (48) and Eq. (51), respectively. The Integral Time of Absolute Errors (ITAE) is used as a cost function to tune the performance of the two controllers, as given in Eq. (63) [51]-[53].

$$ITAE = \int_{t=0}^{t=t_{sim}} tt|e(t)|dt \quad (63)$$

where t_{sim} refers to the total simulation time. The parameters of the SBA are selected as given in Table II.

TABLE II. ALGORITHM PARAMETERS OF SBA

Parameters	Values
Population Size (N)	25
Number of Iterations (T_{max})	40

The convergence behavior of the SBA algorithm to find the design variables of the BSC and the FL is illustrated in Fig. 3 and the design variables are listed in Table III. Fig. 4 depicts the responses of the Maglev system to the step input. The corresponding control signals generated by the proposed controllers are illustrated in Fig. 5.

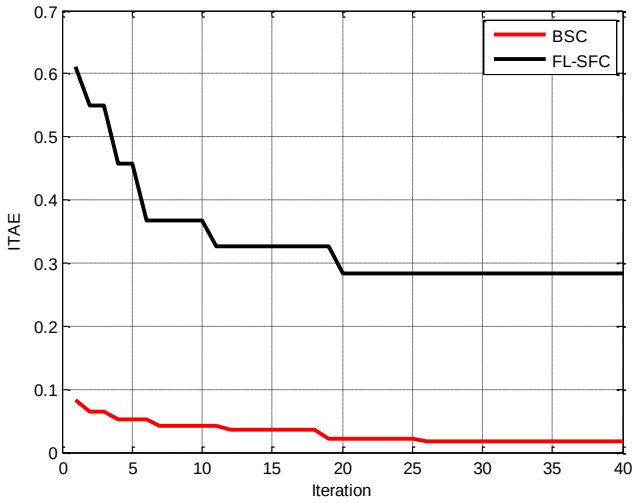

Fig. 3. SBA' convergence

TABLE III. OPTIMAL SETTING OF THE CONTROLLERS

Controller	Parameter	Value
BSC	λ_1	25
	λ_2	30
	λ_3	60
FL-SFC	k_1	80
	k_2	50
	k_3	12

By comparing the two control approaches (BSC and FL-SFC), as shown in Fig. 4 and Table IV, it can be observed that the two controllers are effectively able to control the Maglev system with zero maximum overshoot (Mo) and zero steady-state $error$ $(e_{s.s})$. The results also show that the BSC has achieved a faster tracking response to the desired output than that of the FL-SFC, where the settling time (t_s) is reduced from 1.2s for the FL-SFC to 0.2s for the BSC. Moreover, the BSC improves the ITAE index by 94.19%, where the ITAE index is reduced from 0.2827 for the FL-SFC to 0.0164 for the BSC. Besides, Fig. 5 shows that there is no chattering in the control law of the two controllers.

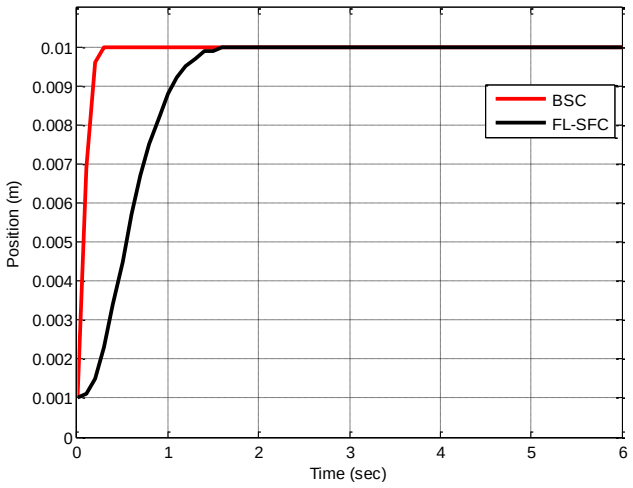

Fig. 4. Position's response of Maglev

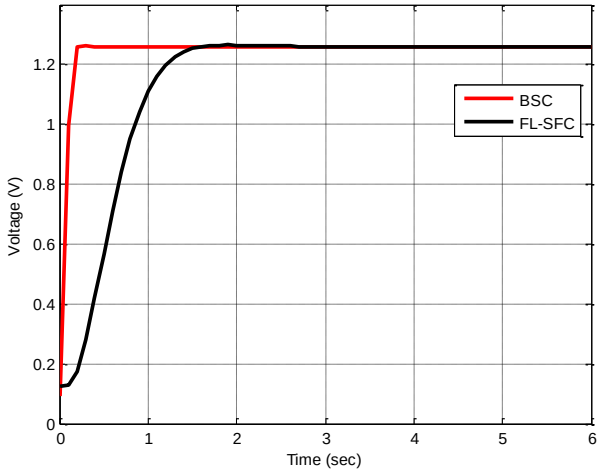

Fig. 5. Control signals

TABLE IV. SYSTEM'S PERFORMANCES

Controller	$t_s(s)$	$e_{s.s}(rad)$	$Mo(\%)$	ITAE
BSC	0.2	0	0	0.0164
FL-SFC	1.2	0	0	0.2827

The robustness ability in terms of rejecting external disturbances for the BSC and the FL-SFC is evaluated by applying an external disturbance to each controlled system after 15 sec of the simulation. Fig. 6 shows the response of the two controlled systems under disturbance. In particular, the recovery time (t_r) and the maximum undershoot (Mu) are used to evaluate the two controllers. The dynamic response of the two controllers in handling the disturbance is reported in Table V. It is clear from Fig. 6 and Table V that the ball's position is recovered from the disturbance to the desired position and remained stable for both controllers. However, BSC has better disturbance rejection where M_u of the BSC was 3 and 19 for FL-SFC. Besides, t_r was 0.05 for the BSC which is less as compared to 0.65of the FL-SFC.

The aforementioned simulation results demonstrate that the BSC is capable of effectively controlling the Maglev in a better manner than that of the FL-SFC for the two studied scenarios, including the normal operation and the influence of the external disturbance.

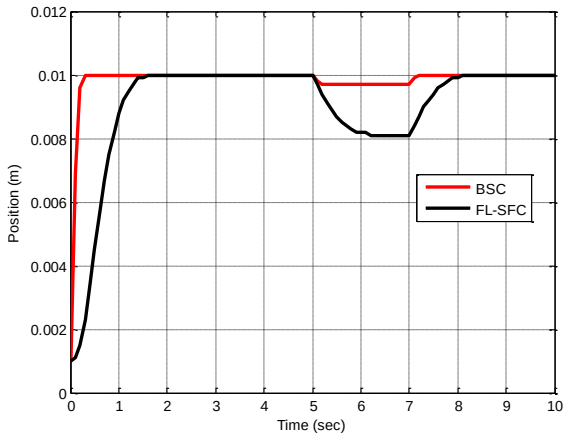

Fig. 6. Position's response of Maglev under external disturbance

TABLE V. SYSTEM'S PERFORMANCES UNDER EXTERNAL DISTURBANCE

Controller	$t_r(s)$	$Mu(\%)$
BSC	0.05	3
FL-SFC	0.65	19

For the purpose of comparison with published paper, the BSC is compared with the result that is obtained in [12]. The result of the comparison is given in Table VI. The two controllers are effectively able to control the Maglev system with zero Mo and zero $e_{s.s}$. The results also show that the BSC has achieved a faster tracking response to the desired output than that of the controller of [12] where t_s is reduced from 0.52 for [12] to 0.2 for the BSC.

TABLE VI. BSC'S PERFORMANCE COMPARISON WITH PUBLISHED WORK

Controller	$t_s(s)$	$e_{s.s}(rad)$	$Mo(\%)$
BSC	0.2	0	0
Ref. [12]	0.52	0	0

V. CONCLUSION

This paper has successfully designed backstepping control (BSC) and a feedback linearization-based state feedback controller (FL-SFC) for the nonlinear model of the magnetic levitation (Maglev) system. Unlike the trial-and-error method, in this work, the swarm bipolar algorithm (SBA) was used as an effective optimization method to optimize the controllers' design parameters. To demonstrate the effectiveness of the synthesized controllers, a numerical comparative simulation based on MATLAB was performed. The results indicated that settling time is reduced from 1.2s for the FL-SFC to 0.2s for the BSC. As a result of that, the BSC improves the ITAE index by 94.19%, where the ITAE index is reduced from 0.2827 for the FL-SFC to 0.0164 for the BSC. The results also showed that the BSC controller can robustly stabilize the system with more desirable performance compared to the FL-SFC. The recovery time was 0.05 for the BSC which is less as compared to 0.65of the FL-SFC.

For future work of this research, another swarm optimization as African vultures' optimization algorithm [54] could be used to select the design parameters of the controllers. Another extension of this study could be by applying a hybrid nonlinear controller such as backstepping sliding mode control [55]-[56] for the Maglev system. Besides, the limitation of the present work is by assumed that all the states of the system are measured. Hence, observer [57]-[60] can be applied to overcome this limitation in the future.

REFERENCES

[1] A. Bizuneh, H. Mitiku, A. O. Salau, and K. Chandran, "Performance analysis of an optimized PID-P controller for the position control of a magnetic levitation system using recent optimization algorithms," *Measurement Sensors*, vol. 33, p. 101228, 2024.

[2] K. Hu, H. Jiang, Q. Zhu, W. Qian, and J. Yang," Magnetic levitation belt conveyor control system based on multi-sensor fusion," *Applied Sciences*, vol.13, no.13, p. 7513, 2023.

[3] P. Kumar, M. Ansari, E. Toyserkani, and M. B. Khamesee, "Experimental implementation of a magnetic levitation system for laser-directed energy deposition via powder feeding additive manufacturing applications," in *Actuators*, vol. 12, no. 6, p. 244, 2023.

[4] S. Ge, A. Nemiroski, K. A. Mirica, C. R. Mace, J. W. Hennek, A. A. Kumar, and G. M. Whitesides, "Magnetic levitation in chemistry, materials science, and biochemistry," *Angewandte Chemie International Edition*, vol. 59, no. 41, pp. 17810-17855, 2020.

[5] R. S. Gopi, S. Srinivasan, K. Panneerselvam, Y. Teekaraman, R. Kuppusamy, and S. Urooj, "Enhanced Model Reference Adaptive Control Scheme for Tracking Control of Magnetic Levitation System," *Energies*, vol. 14, no. 5, p. 1455, 2021.

[6] E. V. Kumar and J. Jerome, "LQR based optimal tuning of PID controller for trajectory tracking of magnetic levitation system," *Procedia Engineering*, vol. 64, pp. 254-264, 2013.

[7] P. Majewski, D. Pawuś, K. Szurpicki, and W. P. Hunek," Toward optimal control of a multivariable magnetic levitation system," *Applied Sciences*, vol. 12, no. 2, p. 674, 2022.

[8] W. Bauer and J. Baranowski, "Fractional PI λ D controller design for a magnetic levitation system," *Electronics*, vol. 9, no. 12, p. 2135, 2020.

[9] S. Dey, J. Dey, and S. Banerjee, "Optimization algorithm based PID controller design for a magnetic levitation system," in *2020 IEEE Calcutta Conference (CALCON)*, pp. 258-262, 2020.

[10] A. Abbas, S. Z. Hassan, T. Murtaza, A. Mughees, T. Kamal, M. A. Khan, and Q. D. Memon, "Design and control of magnetic levitation system," in *2019 International Conference on Electrical, Communication, and Computer Engineering (ICECCE)*, pp. 1-5, 2019.

[11] I. Ahmad, M. Shahzad, and P. Palensky, "Optimal PID control of magnetic levitation system using genetic algorithm," in *2014 IEEE International Energy Conference (ENERGYCON)*, pp. 1429-1433, 2014.

[12] A. M. Benomair, F. A. Bashir, and M. O. Tokhi, "Optimal control based LQR-feedback linearisation for magnetic levitation using improved spiral dynamic algorithm," *2015 20th International Conference on Methods and Models in Automation and Robotics (MMAR)*, pp. 558-562, 2015, doi: 10.1109/MMAR.2015.7283936.

[13] P. Roy, M. Borah, L. Majhi, and N. Singh, "Design and implementation of FOPID controllers by PSO, GSA and PSOGSA for MagLev system," in *2015 International Symposium on Advanced Computing and Communication (ISACC)*, pp. 10-15, 2015.

[14] B. Ataşlar-Ayyildiz and O. Karahan, "Trajectory tracking for the magnetic ball levitation system via fuzzy PID control based on CS algorithm," in *2019 IEEE International Symposium on INnovations in Intelligent SysTems and Applications (INISTA)*, pp. 1-6, 2019.

[15] S. Ekinci, D. Izci, and M. Kayri, "An effective controller design approach for magnetic levitation system using novel improved manta ray foraging optimization," *Arabian Journal for Science and Engineering*, vol. 47, no. 8, pp. 9673-9694, 2022.

[16] N. X. Chiem and L. T Thang, "Synthesis of Hybrid Fuzzy Logic Law for Stable Control of Magnetic Levitation System," *Journal of Robotics and Control (JRC)*, vol. 4, no. 2, pp. 141-148, 2023.

[17] N. F. Al-Muthairi and M. Zribi, "Sliding mode control of a magnetic levitation system," *Mathematical problem in engineering*, vol. 2004, no. 2, pp. 93-107, 2004.

[18] A. Ma'arif, M. Antonio, M. Sadek, E. Umoh, A. Abougarair, and R. Nurindra, "Sliding Mode Control Design for Magnetic Levitation System," *Journal of Robotics and Control (JRC)*, vol. 3, no. 6, pp. 848-853, 2022.

[19] R. Uswarman, S. Istiqphara, and D.H.T. Nugroho, "Sliding mode control with gain scheduled for magnetic levitation system," *Jurnal Ilmiah Teknik Elektro Komputer dan Informatika*, vol. 5, no. 1, pp. 36-43, 2019.

[20] I. Ahmad and M.A. Javaid, "Nonlinear model & controller design for magnetic levitation system," *Recent advances in signal processing, robotics and automation*, pp. 324-328, 2010

[21] S. A. Al-Samarraie, I. I. Gorial, and M. H. Mshari, "An integral sliding mode control for the magnetic levitation system based on backstepping approach," in *IOP Conference Series: Materials Science and Engineering*, vol. 881, no. 1, p. 012136, 2020.

[22] R. A. Kadhim, M. Q. Kadhim, H. Al-Khazrajim, and A. J. Humaidi, "Bee Algorithm Based Control Design for Two-links Robot Arm Systems," *IIUM Engineering Journal*, vol. 25, no.2, pp. 367-380, 2024.

[23] R. M. Naji, H. Dulaimi, and H. Al-Khazraji, "An Optimized PID Controller Using Enhanced Bat Algorithm in Drilling Processes," *Journal Européen des Systèmes Automatisés*, vol. 57, no. 3, pp. 767-772, 2024.

[24] M. A. Al-Ali, O. F. Lutfy, and H. Al-Khazraj, "Investigation of Optimal Controllers on Dynamics Performance of Nonlinear Active Suspension Systems with Actuator Saturation," *Journal of Robotics and Control (JRC)*, vol. 5, no. 4, pp. 1041-1049, 2024.

[25] A. K. Ahmed and H. Al-Khazraji, "Optimal Control Design for Propeller Pendulum Systems Using Gorilla Troops Optimization," *Journal Européen des Systèmes Automatisés*, vol. 56, no. 4, pp. 575-582, 2023.

[26] Z. N. Mahmood, H. Al-Khazraji, and S. M. Mahdi, "PID-based enhanced flower pollination algorithm controller for drilling process in a composite material," in *Annales de Chimie. Science des Materiaux*, vol. 47, no. 2, pp. 91-96, 2023.

[27] H. Al-Khazraji, C. Cole, and W. Guo, "Dynamics analysis of a production-inventory control system with two pipelines feedback," *Kybernetes*, vol. 46, no. 10, pp. 1632-1653, 2017.

[28] H. Al-Khazraji, C. Cole, and W. Guo, "Analysing the impact of different classical controller strategies on the dynamics performance of production-inventory systems using state space approach," *Journal of Modelling in Management*, vol. 13, no. 1, pp. 211-235, 2018.

[29] E. Oumaymah, O. Abdellah, B. Omar, and E. B. Lhoussain, "Backstepping Design Control Applied to the Wind PMSG Generator and Grid Connection Using A Multilevel Inverter," *2021 8th International Conference on Electrical and Electronics Engineering (ICEEE)*, pp. 136-141, 2021.

[30] M. T. Vo, M. T. Nguyen, T. T. H. Le, V. Do Tran, D. T. Tran, T. M. N. Nguyen, and V. T. Ngo, "Back-stepping control for rotary inverted pendulum," *Journal of Technical Education Science*, vol. 15, no. 4, pp. 93-101, 2020`.

[31] H. Al-Khazraji, R. M. Naji, and M. K. Khashan "Optimization of Sliding Mode and Back-Stepping Controllers for AMB Systems Using Gorilla Troops Algorithm," *Journal Européen des Systèmes Automatisés*, vol. 57, no. 2, pp. 417–424, 2024.

[32] M. S. Xavier, A. J. Fleming, and Y. K. Yong, "Nonlinear estimation and control of bending soft pneumatic actuators using feedback linearization and UKF," *IEEE/ASME Transactions on Mechatronics*, vol. 27, no. 4, pp. 1919-1927, 2022.

[33] M. Vesović, R. Jovanović, and N. Trišović, "Control of a DC motor using feedback linearization and gray wolf optimization algorithm," *Advances in Mechanical Engineering*, vol. 14, no. 3, 2022.

[34] A. Hache, M. Thieffry, M. Yagoubi, and P. Chevrel, "Control-Oriented Neural State-Space Models for State-Feedback Linearization and Pole Placement," in *2022 10th International Conference on Systems and Control (ICSC)*, pp. 429-434, 2022.

[35] H. Li, Z. Wang, Z. Xu, X. Wang, and Y. Hu, "Feedback linearization based direct torque control for IPMSMs," *IEEE Transactions on Power Electronics*, vol. 36, no. 3, pp. 3135-3148, 2020.

[36] H. Al-Khazraji, C. Cole, and W. Guo, "Multi-objective particle swarm optimisation approach for production-inventory control systems," *Journal of Modelling in Management*, vol. 13, no. 4, pp. 1037-1056, 2018.

[37] A. K. Ahmed, H. Al-Khazraji, and S. M. Raafat, "Optimized PI-PD Control for Varying Time Delay Systems Based on Modified Smith Predictor," *International Journal of Intelligent Engineering & Systems*, vol. 17, no. 1, pp. 331-342, 2024.

[38] H. A. Azzawi, N. M. Ameen, and S. A. Gitaffa, "Comparative Performance Evaluation of Swarm Intelligence-Based FOPID Controllers for PMSM Speed Control," *Journal Européen des Systèmes Automatisés*, vol. 56, no. 3, pp. 475-482, 2023.

[39] X. Zhao, R. Ogawa, and S. C. Sung, "On Searching Optimal Worker Assignment in Multi-stage Production Lines," in *The International Conference on Smart Manufacturing, Industrial & Logistics Engineering (SMILE)*, pp. 205-211, 2023.

[40] H. Al-Khazraji, A. R. Nasser, and S. Khlil, "An intelligent demand forecasting model using a hybrid of metaheuristic optimization and deep learning algorithm for predicting concrete block production," *IAES International Journal of Artificial Intelligence*, vol. 11, no. 2, pp. 649-657, 2022.

[41] H. Al-Khazraji, W. Guo, and A. J. Humaidi, "Improved Cuckoo Search Optimization for Production Inventory Control Systems," *Serbian Journal Of Electrical Engineering*, vol. 21, no. 2, pp. 187-200, 2024.

[42] H. AL-Khazraji, C. Cole, and W. Guo, "Optimization and simulation of dynamic performance of production–inventory systems with multivariable controls," *Mathematics*, vol. 9, no. 5, 2021.

[43] F. R Yaseen, M. Q. Kadhim, H. Al-Khazraji, and A. J. Humaidi, "Decentralized Control Design for Heating System in Multi-Zone Buildings Based on Whale Optimization Algorithm," *Journal Européen des Systèmes Automatisés*, vol. 57, no. 4, pp. 981-989, 2024.

[44] H. Al-Khazraji, S. Khlil, and Z. Alabacy, "Industrial picking and packing problem: Logistic management for products expedition," *Journal of Mechanical Engineering Research and Developments*, vol. 43, no. 2, pp. 74-80, 2020.

[45] S. Khlil, H. Al-Khazraji, and Z. Alabacy, "Solving assembly production line balancing problem using greedy heuristic method," in *IOP Conference Series: Materials Science and Engineering*, vol. 745, no. 1, p. 012068, 2020.

[46] H. Al-Khazraji, "Optimal Design of a Proportional-Derivative State Feedback Controller Based on Meta-Heuristic Optimization for a Quarter Car Suspension System," *Mathematical Modelling of Engineering Problems*, vol. 9, no. 2, pp. 575-582, 2022.

[47] H. Al-Khazraji K. Al-Badri, R. Al-Majeez, and A. J. Humaidi, "Synergetic Control Design Based Sparrow Search Optimization for Tracking Control of Driven-Pendulum System," *Journal of Robotics and Control (JRC)*, vol. 5, no. 5, pp. 1549-1556, 2024.

[48] N. M. Alyazidi, A. M. Hassanine, M. S. Mahmoud, and A. Ma'arif, "Enhanced Trajectory Tracking of 3D Overhead Crane Using Adaptive Sliding-Mode Control and Particle Swarm Optimization," *Journal of Robotics and Control (JRC)*, vol. 5, no. 1, pp. 253-262, 2024.

[49] H. Al-Khazraji, K. Albadri, R. Almajeez, and A. J. Humaidi, "Synergetic Control-Based Sea Lion Optimization Approach for Position Tracking Control of Ball and Beam System," *International Journal of Robotics and Control Systems*, vol. 4, no. 4, pp. 1547-1560, 2024.

[50] P. D. Kusuma and A. Dinimaharawati, "Swarm Bipolar Algorithm: A Metaheuristic Based on Polarization of Two Equal Size Sub Swarms," *International Journal of Intelligent Engineering & Systems*, vol. 17, no. 2, 2024.

[51] M. A. AL-Ali, O. F. Lutfy, and H. Al-Khazraj, "Comparative Study of Various Controllers Improved by Swarm Optimization for Nonlinear Active Suspension Systems with Actuator Saturation," *International Journal of Intelligent Engineering & Systems*, vol. 17, no. 4, pp. 870-881, 2024.

[52] Z. N. Mahmood, H. Al-Khazraji, and S. M. Mahdi, "Adaptive control and enhanced algorithm for efficient drilling in composite materials," *Journal Européen des Systèmes Automatisés*, vol. 56, no. 3, pp. 507-512, 2023.

[53] S. R. Gampa, S. K. Mangipudi, K. Jasthi, P. Goli, D. Das, and V. Balas, "Pareto optimality based PID controller design for vehicle active suspension system using grasshopper optimization algorithm," *Journal of Electrical Systems and Information Technology*, vol. 9, no. 1, p. 24, 2022.

[54] M. S. Abed, O. F. Lutfy, and Q. F. Al-Doori, "Online path planning of mobile robots based on African vultures optimization algorithm in unknown environments," *Journal Européen des Systèmes Automatisés*, vol. 55, no. 3, pp. 405-412, 2022.

[55] A. Ma'arif, M. A. M. Vera, M. S. Mahmoud, S. Ladaci, A. Çakan, and J. N. Parada, "Backstepping sliding mode control for inverted pendulum system with disturbance and parameter uncertainty," *Journal of Robotics and Control (JRC)*, vol. 3, no. 1, pp. 86-92, 2022.

[56] F. E. Z. Lamzouri, E. M. Boufounas, M. Hanine, and A. E. Amrani, "Optimised backstepping sliding mode controller with integral action for MPPT-based photovoltaic system using PSO technique," *International Journal of Computer Aided Engineering and Technology*, vol. 18, pp. 97-109, 2023.

[57] N. S. Mahmood, A. J. Humaidi, R. S. Al-Azzawi, and A. Al-Jodah, "Extended state observer design for uncertainty estimation in electronic throttle valve system," *International Review of Applied Sciences and Engineering*, vol. 15, no. 1, pp. 107-115, 2024.

[58] C. E. Martínez Ochoa, I. O. Benítez González, A. O. Cepero Díaz, J. R. Nuñez-Alvarez, C. G. Miguélez-Machado, and Y. Llosas Albuerne, "Active disturbance rejection control for robot manipulator," *Journal of Robotics and Control (JRC)*, vol. 3, no. 5, pp. 622-632, 2022.

[59] N. A. Alawad, A. J. Humaidi, and A. S. Alaraji, "Observer sliding mode control design for lower exoskeleton system: Rehabilitation case," *Journal of Robotics and Control (JRC)*, vol. 3, no. 4, pp. 476-482, 2022.

[60] M. A. Mossa, H. Echeikh, and A. Ma'arif, "Dynamic Performance Analysis of a Five-Phase PMSM Drive Using Model Reference Adaptive System and Enhanced Sliding Mode Observer," *Journal of Robotics and Control (JRC)*, vol. 3, no. 3, pp. 289-308.